The Solid-state "Bayer Process"-inspired Valorization Route: Adding a Sodium Alumino-silicate to the Precursor

Fábio Oliveira[1], Tobias Hertel[2] and Yiannis Pontikes[3]
1. PhD candidate
2. Post-doctoral researcher
3. Professor
KU Leuven, Department of Materials Engineering, Leuven, Belgium
Corresponding author: fabio.oliveira@kuleuven.be

Abstract

Despite the potential of re-use in many sectors, less than 3 % of the annually produced bauxite residue (BR) is in some way valorized, with the rest being usually stored in disposal areas. This work aims to increase the valorization of BR by producing dense monoliths through alkali-activation followed by hydrothermal curing in an autoclave, a process which is believed to be simple, robust and most likely of low CAPEX and OPEX. The solid precursors, BR and an alumino-silicate by-product from the spent potlining treatment by the Low Caustic Leaching and Liming process, named LCLL ash, were dry mixed in contents of 80 and 100 wt% of BR and 0 and 20 wt% of LCLL ash. Na-silicate was added as an alkaline activator, and the final blend was press-shaped at 50 MPa for 1 min to obtain prismatic specimens of 6x1.5x1.5 cm^3. Curing took place in an autoclave at 220 °C for 24 h. X-ray diffraction showed that the hydrothermal curing promoted the dissolution of quartz and gibbsite, and the formation of zeolites (and zeolite-type phases), such as cancrinite and analcime. The compressive strength of the autoclaved specimens was six times higher than that of the specimens cured at room temperature, and the addition of LCLL ash significantly improved the strength gain (from 31 MPa in the sample containing only BR, to 40 MPa in the sample with LCLL ash). An upscaling of such process seems feasible, even within the premises of alumina plants, as the knowledge on such processing or the required infrastructure (e.g., autoclaves) is available within the industry. Final products can be tiles, bricks, or other building elements.

Keywords: Bauxite residue, Red mud, Dense monoliths, Autoclave curing, Alumina plant residues.

1. Introduction

The Bayer process is the principal industrial approach to produce alumina, characterized by the digestion of the bauxite ore with caustic soda and further precipitation of alumina (oxy)hydroxide [1]. A significant portion of the bauxite does not dissolve during the process and is usually discarded and stored in disposal areas, receiving the name of bauxite residue (BR) or red mud. The production of 1 t of alumina generates 1-1.5 t of bauxite residue [2], and as the production of alumina to produce aluminium increases, so does the generation of bauxite residue. According to the International Aluminium Institute (IAI) [3], the production of BR in 2017 was close to 160 Mt and is expected to increase to 220 Mt by 2040, resulting in a global inventory of 8 billion tonnes of BR. The residue is accumulated in disposal areas, and poses potential risks for ecosystems and human health due to the high alkalinity in combination with its fine particle size distribution [2,4]. Therefore, over the last decades, efforts have been made to find applications for this material.

Some of the most attractive areas for the use of BR are the following: construction materials [5–9], metals recovery [10], soil amelioration [9], road constructions [11], pigments and glass-ceramics [2]. Despite the numerous alternatives, however, only about 3% of the total mass of BR

available is used, with some of the major barriers being its high alkalinity and moisture content [2].

One possible and promising way of using bauxite residue is in the production of alkali-activated materials (AAM), which can benefit from the BR's chemical composition (Si, Al, Ca and Fe) and inherent alkalinity. AAM's are produced from a mostly amorphous precursor, usually an aluminum silicate, and an alkaline activator [12], resulting in a material with properties that can be superior to those of conventional binders [13], such as high early strength and resistance to chemical attack. Moreover, their production can result in a lower carbon footprint in comparison to conventional binders [14], as there is no need for calcination at elevated temperatures as in the case of Portland cement clinker. The major drawback related to the use of BR to produce AAM is its low reactivity, which is the reason why many researches have used BR merely as a minor addition (<20 wt%) to other precursors. Alternatives to overcome this challenge usually require the use of high temperatures (> 1000 °C), significant energy consumption and/or expensive/high-carbon footprint additions.

A conceivable and more environmentally friendly process is through hydrothermal curing at temperatures below 300 °C and under high pressure, which can increase the dissolution of the phases in the BR, and hence its reactivity. A successful example of this approach is the patent developed by Hertel and Pontikes [15], in which the inventors produced 100 wt% BR monoliths with compressive strengths up to 20 MPa. The bauxite residue was activated with sodium silicate solution and samples were put into shape using pressures of 19 and 50 MPa. Specimens were hydrothermally cured in autoclave at 220 or 260 °C and the respective steam pressures. After autoclaving, quartz and gibbsite, which were present in the precursor, showed a significant decrease in intensity in the XRD patterns, indicating that these phases dissolved under hydrothermal curing. The use of industrial clay and kaolin as additives increased the reactivity, resulting in better mechanical performance. A manuscript has been submitted based on the outcomes of the patent [16].

The aforementioned process was coined Solid-state "Bayer Process"-inspired Valorization Route, as, similarly to the Bayer process, it makes use of an alkaline agent to get the raw materials to react in an autoclave, with the major differences (apart from the resulting products) being the very low liquid content and the press-shaping of the monoliths. The process was put into practice in this paper using bauxite residue and a by-product from an aluminium electrolysis plant, aiming to investigate the synergy between residues from the same producer. The methodology consisted in mixing the raw materials and press-shaping specimens followed by hydrothermal curing in an autoclave at 220 °C for 24 h. The specimens were characterized before and after autoclaving in terms of mineralogy and compressive and flexural strength.

2. Materials and Methods

Bauxite residue and a by-product from the Low Caustic Leaching and Liming process, named LCLL ash, were supplied by Rio Tinto and used as raw materials in this research. The LCLL ash is a sodium aluminosilicate and more information on how it is obtained can be found elsewhere [17,18]. Both materials were dried at 105 °C until constant mass, deagglomerated using a disk mill (Pulverisette 13, Fritsch) and characterized in terms of chemistry, mineralogy and physical parameters.

Chemistry was determined by Wavelength Dispersive X-ray fluorescence (WDXRF) in a Bruker S8 Tiger (4 kW Rh system) and analyzed in the software Uniquant 5 (Omega Data System BV). Loss on ignition was determined by means of thermogravimetric analysis using a TA Instruments DSC SDT Q600 Thermogravimetric Analyzer, at a heating rate of 5 °C/min from ambient temperature to 1000 °C in N_2 atmosphere. Mineralogy was qualitatively accessed by X-ray

diffraction (XRD) on a D2 Phaser (Bruker) with an acceleration voltage of 30 kV and a current of 10 mA. Diffractograms were recorded in a range from 5 to 65 º2θ with a measuring time of 5 s/step and analyzed using the software DIFFRAC.EVA with the PDF-4+ database from the International Centre for Diffracton Data. The particle size distribution (PSD) was measured by Laser Diffraction using a Beckmann Coulter device. Prior to the measurement, the dried samples were immersed in ethanol and deagglomerated using ultrasound. The specific surface area (SSA) was accessed by BET on the basis of nitrogen adsorption using a Tristar II analyzer (Micromeritics).

Two mix designs were defined (Table 1): 100BR (containing only bauxite residue) and 80BR20LCLL (80 wt% of BR and 20 wt% of LCLL ash). A Na-silicate with SiO_2/Na_2O ratio of 1.6 and water content of 65 wt% was used as alkaline activator. The liquid-to-solid ratio (L/S) was 0.15 g/g for all mix designs.

Table 1. Mix designs.

Mix design	Solids (wt%)		Na-silicate (SiO_2/Na_2O=1.6, 65 % H_2O)
	BR	LCLL ash	L/S (g/g)
100BR	100	0	0.15
80BR20LCLL	80	20	0.15

To ensure homogeneity of the mix, mixing was performed in a laboratory Eirich intensive mixer (model EL1). First, the dry solids were mixed together for 30 s at 500 rpm for homogenization, then the alkaline solution was added while mixing for additional 30 s at the same speed. Next, mixing continued at a speed of 5000 rpm for a total of 5 min, with a one minute break after 2.5 min to detach the material from the walls of the vessel and achieve a better homogenization. Samples of the final blend were taken and kept in a plastic bag for XRD analysis before hydrothermal curing.

After mixing, prismatic specimens of 6x1.5x1.5 cm^3 (Figure 1a) were produced by pressing at 50 MPa for 60 s using a hydraulic automatic laboratory press (Mignon SSN/EA, Nannetti). For the autoclaving curing, the shaped specimens were placed inside a 2 liters vessel with 100 ml of deionized water (a steel support was used to avoid the specimens to touch the water), and kept closed in a laboratory oven at 220 °C for 24 hours. After this time, the oven was turned off and let to cool to ambient temperature. The vessel was then opened and the specimens were wrapped in foil and kept at room temperature until the day of testing.

The specimens were tested on strength seven days after production, using an Instron machine (model 5985) coupled with a 250 kN load cell. Flexural strength was measured first, breaking the prismatic specimens in half; compressive strength was measured afterwards using each half. Due to the small dimensions of the specimens, supports were used to accurately measure the strength (Figure 1b and (Figure 1c). Finally, fragments of the tested specimens were ground using pestle and mortar and sieved below 80 µm for XRD analysis. A flowsheet of the methodology is presented in Figure 2.

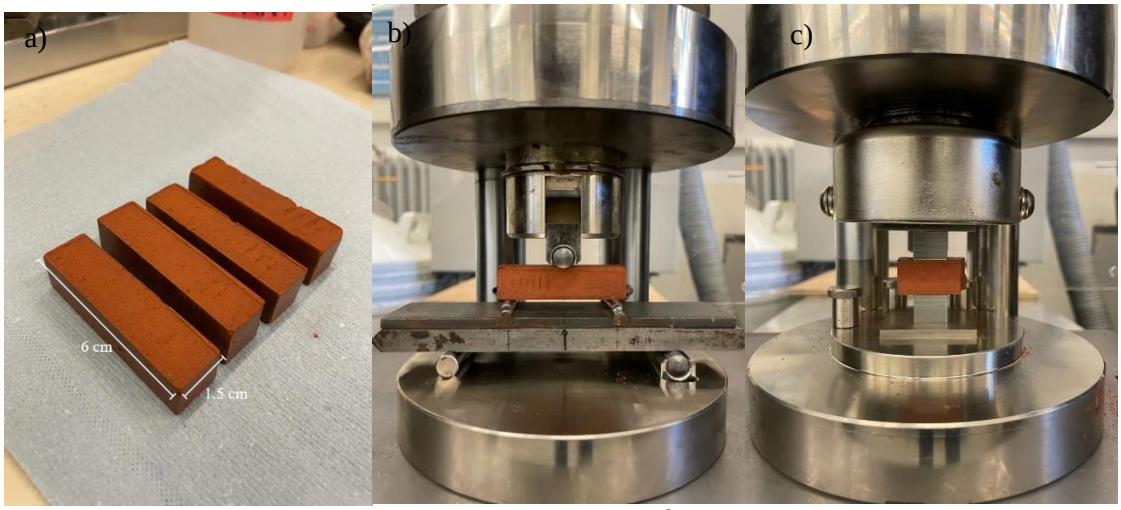

Figure 1. a) Prismatic specimens of 6x1.5x1.5 cm^3, b) configuration for the flexural strength measured by three point bending test, c) configuration for the compressive strength test.

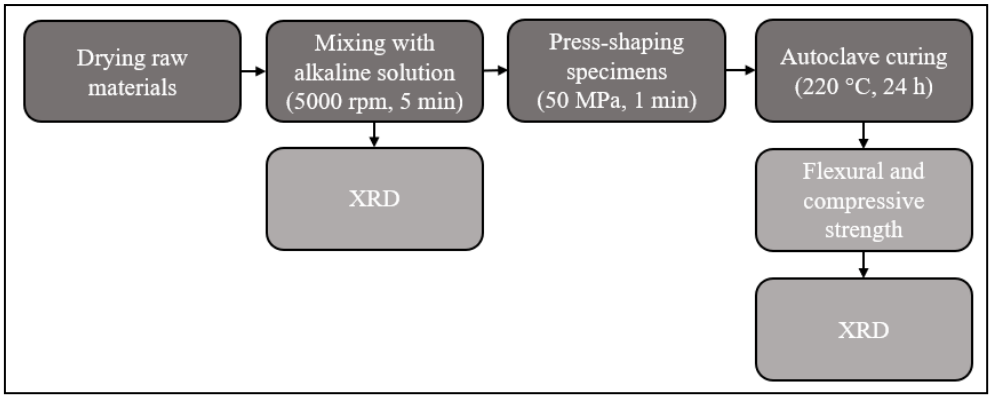

Figure 2. Flowsheet of the methodology.

3. Results

3.1 Characterization of Raw Materials

The chemistry and mineralogy of the BR and the LCLL ash are presented in Table 2 and Figure 3. The high amount of iron in the BR comes from hematite (Fe_2O_3) and goethite (FeO(OH)), which will likely remain inert during hydrothermal curing. Sodalite ($Na_8[Al_6Si_6O_{24}]OH_2.nH_2O$), boehmite (AlO(OH)), gibbsite ($Al(OH)_3$) and quartz (SiO_2) are present in minor amounts and might dissolve during autoclave processing. Illite ($K_{0.65}Al_2[Al_{0.65}Si_{3.35}O_{10}](OH)_2$), anatase ($TiO_2$), calcite ($CaCO_3$), rutile ($TiO_2$) and katoite ($Ca_3Al_2(SiO_4)(OH)_8$) were also detected. The LCLL ash is majorly composed by Al_2O_3 and SiO_2. Major phases are nepheline ($NaAlSiO_4$) and corundum (Al_2O_3), with diaoyudaoite ($NaAl_{11}O_{17}$), graphite (C), quartz and fluorite (CaF_2) present in minor amounts. The physical characterization (Table 3) has shown that the BR is very fine, with a d_{50} of 1.2 μm and a relatively high SSA of 13.9 m^2/g, in accordance with values found in literature [19]; the LCLL is much coarser, with a d_{50} of 58.1 μm and a SSA of 5 m^2/g.

Table 2. Chemistry of the bauxite residue and the LCLL ash, obtained by XRF.

Compound	BR (wt%)	LCLL ash (wt%)
Fe_2O_3	51.5	4.0
Al_2O_3	16.4	31.7
SiO_2	11.0	30.4
TiO_2	5.4	0.9
Na_2O	5.1	9.1
CaO	2.3	6.1
Others	0.1	2.9
LOI	8.3	14.5

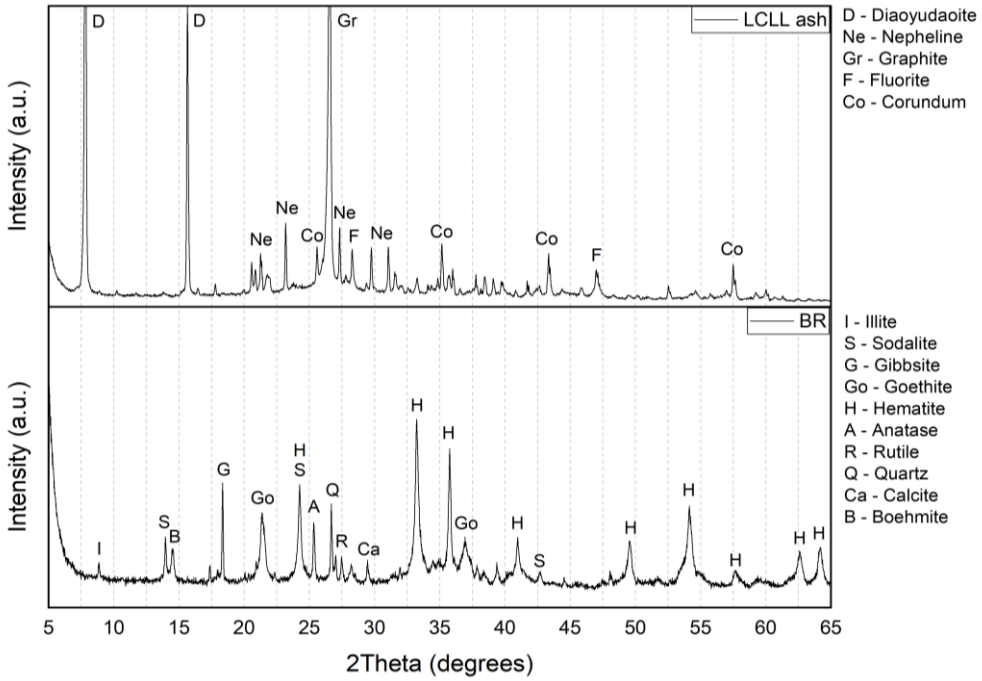

Figure 3. XRD patterns for the bauxite residue and LCLL ash.

Table 3. Physical parameters of the BR and the LCLL ash.

Material	SSA (m^2/g)	PSD (μm)		
		d_{10}	d_{50}	d_{90}
BR	13.9	0.3	1.2	9.6
LCLL ash	5	6.8	58.1	351.8

3.2 Characterization of Specimens

3.2.1 Mineralogy

Figure 4a (lower graph) shows the diffractograms of the 100BR specimens before and after autoclave curing (black and red lines, respectively). Figure 4b (upper graph) shows the subtraction of the two patterns, where negative values indicate dissolution of phases and positive values, formation of phases. The peaks for hematite and goethite remained the same after autoclaving, indicating that such phases are rather inert in the current hydrothermal conditions. Gibbsite and

quartz dissolved, releasing aluminate and silica species that reacted with the Na-silicate to form cancrinite, according to the proposed Equation (1) [20]. Such reaction is common in the digestion of the bauxite through the Bayer process in alumina refineries, in which the dissolution of quartz is unwanted, as it increases the consumption of soda and alumina [1]; in our case it is beneficial as it increases the reactivity of the precursor. Moreover, cancrinite may also have formed through a transformation from sodalite under high temperatures (> 145 °C) [1], but this is difficult to confirm due to superposition of peaks.

$$6Al(OH)_4^- + 6SiO_3^{2-} + 6Na^+ + 2OH^- \rightarrow Na_8[AlSiO_4]_6OH_2.nH_2O + (6\text{-}n)H_2O + 12OH^- \quad (1)$$

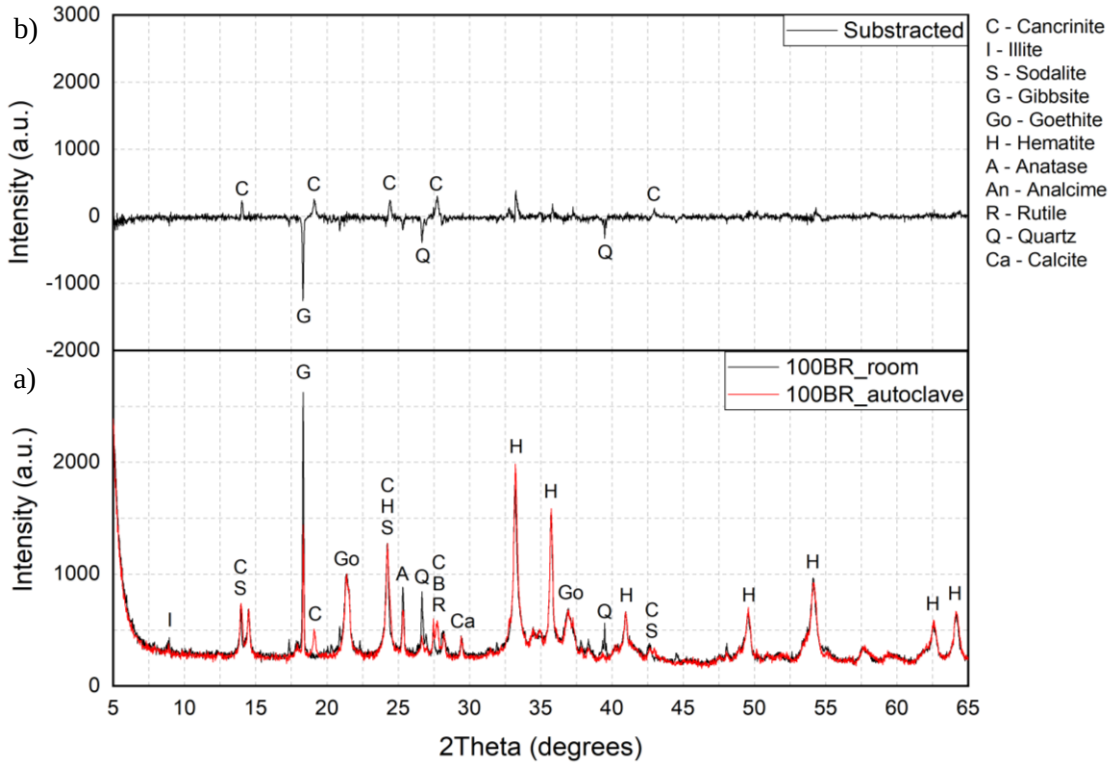

Figure 4 a) XRD patterns of the 100BR samples before and after autoclaving (lower graph), b) subtraction of the two patterns, in which negative values indicate dissolution of phases, and positive values, formation of phases (upper graph).

Similarly, the 80BR20LCLL samples also presented the dissolution of gibbsite and quartz to form mostly cancrinite after autoclaving (Figure 5). Small peaks of the zeolite analcime ($NaAlSi_2O_6.H_2O$) were also detected, likely due to the higher amount of Na, Al and Si in the LCLL ash in comparison to the BR. The formation of analcime opens opportunities for a variety of applications, including adsorption technologies for treatment of liquid streams and heterogeneous catalysis [21]. Other benefits of having zeolites in building materials can include improvement of durability and better resistance to cracking by self-shrinkage [22]. Equation (2) is suggested for the formation of analcime [20].

$$Al(OH)_4^- + 2H_2SiO_4^{2-} + Na^+ \rightarrow NaAlSi_2O_6.H_2O + 4OH^- + 2H_2O \quad (2)$$

Moreover, the peaks of diaoyudaoite increased, which might indicate that more of this phase has formed during autoclaving. According to Lewandowski [23], sodium may attack the alumina to form $Na_2O\text{-}11Al_2O_3$.

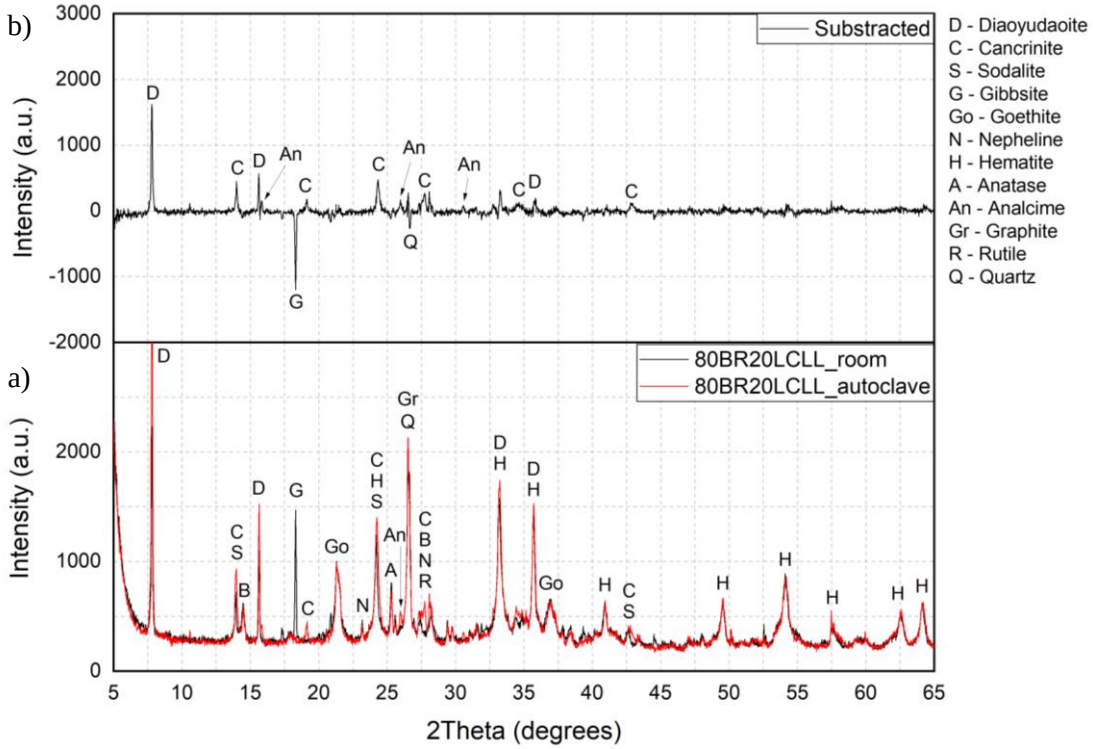

Figure 5. a) XRD patterns of the 80BR20LCLL samples before and after autoclaving (lower graph), b) subtraction of the two patterns, in which negative values indicate dissolution of phases, and positive values, formation of phases (upper graph).

3.2.2 Mechanical Performance

Results for compressive and flexural strength are presented in Figure 6, in which 100BR_room indicates samples that were not autoclaved and kept at room temperature wrapped in foil. When comparing the non-autoclaved with the autoclaved 100BR specimens, the mechanical performance was improved significantly after hydrothermal curing, being six times higher for compressive strength and three times higher for flexural strength. The formation of cancrinite is likely responsible for the strength gain, as feldspathoids are believed to improve the mechanical performance of geopolymers [20,24].

The addition of LCLL ash to the composition improved the mechanical performance even further: the compressive strength was 33 % higher and the flexural strength 55 % higher in comparison to the specimens containing only BR (ANOVA analysis for compressive strength concluded that the means are significantly different at a confidence level of 0.05 (p-value = 0.01)). The formation of analcime might have played a role in the strength gain, as researches have shown that adding natural zeolites in concrete can improve the compressive strength, which will depend on the content since they can increase the porosity significantly [25,26].

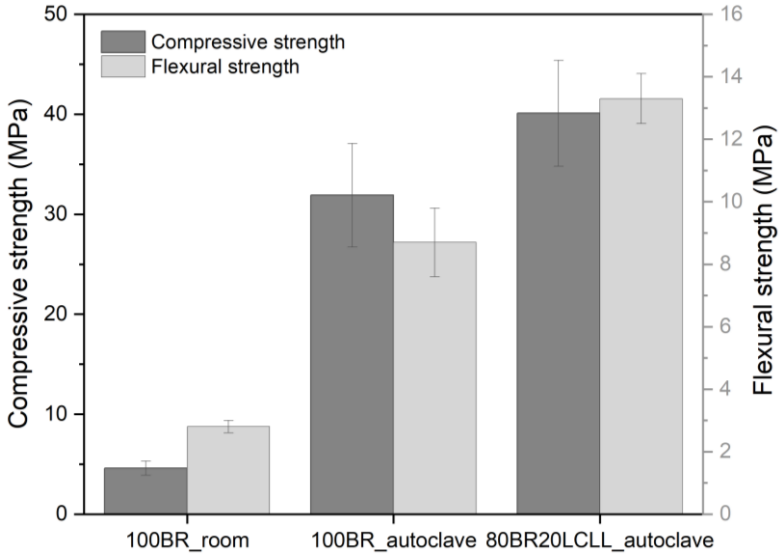

Figure 6. Compressive and flexural strength results. For each mix design, compressive strength was calculated based on eight samples, whereas the flexural strength was determined based on four samples.

4. Conclusion

In this paper, a valorization route for the bauxite residue, inspired by the Bayer process, was presented. The route is characterized by the alkali activation of solids, followed by the press-shaping of specimens and hydrothermal curing in an autoclave. Similarly to the Bayer process, phases such as gibbsite and quartz dissolve during the hydrothermal curing to form products that contribute to the mechanical performance of the final material. The aim of the paper was to investigate the output of the process and the synergy between two aluminium industry by-products from the same producer:bauxite residue and LCLL ash, the latter obtained from Spent Pot lining treatment plant.

It was shown that for specimens containing only bauxite residue, and activated with a very low amount of Na-silicate (L/S=0.15 g/g), the autoclave curing improved the compressive strength by a factor of six. The formation of cancrinite is suggested as the main responsible phase for the strength gain. The use of additives has proven to be able to improve the mechanical performance even further. The addition of 20 wt% of LCLL ash increased the compressive and flexural strengths in 33 % and 55 %, respectively, in comparison to the specimens containing only BR. Apart from cancrinite, the zeolite analcime was formed, which opens opportunities for new applications other than building materials, such as adsorption technologies.

The Solid-state “Bayer Process”-inspired Valorization Route has proven to be a viable alternative to re-use significant amounts of bauxite residue. Moreover, the addition of other wastes from alumina refineries to the precursor can boost the mechanical properties of the final monoliths, which can be brick, tiles, panels and other building elements. The process is simple, robust and likely of low CAPEX and OPEX, which turns it feasible to be implemented even in alumina refineries. The use of common and readily available materials (e.g., quartz sand, clay, construction and demolition waste) as additives can be suitable to increase the reactivity of the precursor in the autoclave and to trigger the formation of reaction products (such as C-(A)-S-H phases) that can improve the mechanical performance even further.

Acknowledgements

The authors would like to thank Rio Tinto for providing the raw materials used in this research. We are also grateful to Laurent Birry, Sébastien Fortin and Santiago Ramirez for the discussions prior and during the writing of this paper.

5. References

1. B.E. Raahauge, F.S. Williams, eds., *Smelter grade alumina from bauxite: history, best practices, and future challenges*, Springer, 2022. https://doi.org/10.1007/978-3-030-88586-1.
2. K. Evans, The History, Challenges, and New Developments in the Management and Use of Bauxite Residue, *J. Sustain. Metall.* 2 (2016) 316–331. https://doi.org/10.1007/s40831-016-0060-x.
3. International Aluminium Institute, Maximising the use of Bauxite Residue in Cement, 2020.
4. G. Power, M. Gräfe, C. Klauber, Bauxite residue issues: I. Current management, disposal and storage practices, *Hydrometallurgy*. 108 (2011) 33–45. https://doi.org/10.1016/j.hydromet.2011.02.006.
5. Y. Pontikes, G.N. Angelopoulos, Bauxite residue in cement and cementitious applications: Current status and a possible way forward, Resources, *Conservation and Recycling*. 73 (2013) 53–63. https://doi.org/10.1016/j.resconrec.2013.01.005.
6. M. Singh, S.N. Upadhayay, P.M. Prasad, Preparation of special cements from red mud, *Waste Management*. 16 (1996) 665–670. https://doi.org/10.1016/S0956-053X(97)00004-4.
7. P.E. Tsakiridis, S. Agatzini-Leonardou, P. Oustadakis, Red mud addition in the raw meal for the production of Portland cement clinker, *Journal of Hazardous Materials*. 116 (2004) 103–110. https://doi.org/10.1016/j.jhazmat.2004.08.002.
8. I. Vangelatos, G.N. Angelopoulos, D. Boufounos, Utilization of ferroalumina as raw material in the production of Ordinary Portland Cement, *Journal of Hazardous Materials*. 168 (2009) 473–478. https://doi.org/10.1016/j.jhazmat.2009.02.049.
9. R.K. Paramguru, P.C. Rath, V.N. Misra, TRENDS IN RED MUD UTILIZATION – A REVIEW, *Mineral Processing and Extractive Metallurgy Review*. 26 (2004) 1–29. https://doi.org/10.1080/08827500490477603.
10. E. Erçağ, R. Apak, Furnace smelting and extractive metallurgy of red mud: recovery of TiO_2, Al_2O_3 and pig iron, *J. Chem. Technol. Biotechnol.* 70 (1997) 241–246. https://doi.org/10.1002/(SICI)1097-4660(199711)70:3<241::AID-JCTB769>3.0.CO;2-X.
11. W.K. Biswas, D. Cooling, Sustainability Assessment of Red Sand as a Substitute for Virgin Sand and Crushed Limestone: Sustainability Assessment of Red Sand, *Journal of Industrial Ecology*. 17 (2013) 756–762. https://doi.org/10.1111/jiec.12030.
12. M.T. Marvila, A.R.G. de Azevedo, C.M.F. Vieira, Reaction mechanisms of alkali-activated materials, *Rev. IBRACON Estrut. Mater.* 14 (2021) e14309. https://doi.org/10.1590/s1983-41952021000300009.
13. T. Hertel, Y. Pontikes, Geopolymers, inorganic polymers, alkali-activated materials and hybrid binders from bauxite residue (red mud) – Putting things in perspective, *Journal of Cleaner Production*. 258 (2020) 120610. https://doi.org/10.1016/j.jclepro.2020.120610.
14. G. Habert, J.B. d'Espinose de Lacaillerie, N. Roussel, An environmental evaluation of geopolymer based concrete production: reviewing current research trends, *Journal of Cleaner Production*. 19 (2011) 1229–1238. https://doi.org/10.1016/j.jclepro.2011.03.012.
15. T. Hertel, Y. Pontikes, Non-fired monoloths, US11111179B2, 2019.
16. T. Hertel, Y. Pontikes, D. Sakellariou, The solid-state "Bayer process"-inspired valorisation route: an add-on option to transform bauxite residue into monoliths, Submitted to the *Journal of Sustainable Metallurgy*. (2021).
17. V. Brial, H. Tran, L. Sorelli, D. Conciatori, C.M. Ouellet-Plamondon, Evaluation of the reactivity of treated spent pot lining from primary aluminum production as cementitious

materials, Resources, *Conservation and Recycling*. 170 (2021) 105584. https://doi.org/10.1016/j.resconrec.2021.105584.
18. L. Birry, S. Leclerc, S. Poirier, The LCL&L Process: A Sustainable Solution for the Treatment and Recycling of Spent Potlining, in: E. Williams (Ed.), *Light Metals* 2016, John Wiley & Sons, Inc., Hoboken, NJ, USA, 2016: pp. 467–471. https://doi.org/10.1002/9781119274780.ch77.
19. K. Snars, R.J. Gilkes, Evaluation of bauxite residues (red muds) of different origins for environmental applications, *Applied Clay Science*. 46 (2009) 13–20. https://doi.org/10.1016/j.clay.2009.06.014.
20. T. Hertel, Binders and Monoliths from Bauxite Residue (Red Mud), PhD Thesis, KU Leuven, 2020.
21. D. Novembre, D. Gimeno, Synthesis and characterization of analcime (ANA) zeolite using a kaolinitic rock, *Sci Rep*. 11 (2021) 13373. https://doi.org/10.1038/s41598-021-92862-0.
22. N.-Q. Feng, G.-F. Peng, Applications of natural zeolite to construction and building materials in China, *Construction and Building Materials*. 19 (2005) 579–584. https://doi.org/10.1016/j.conbuildmat.2005.01.013.
23. D.A. Lewandowski, *Design of Thermal Oxidation Systems for Volatile Organic Compounds*, 2017.
24. K. Komnitsas, D. Zaharaki, V. Perdikatsis, Geopolymerisation of low calcium ferronickel slags, *J Mater Sci*. 42 (2007) 3073–3082. https://doi.org/10.1007/s10853-006-0529-2.
25. D. Nagrockiene, G. Girskas, Research into the properties of concrete modified with natural zeolite addition, *Construction and Building Materials*. 113 (2016) 964–969. https://doi.org/10.1016/j.conbuildmat.2016.03.133.
26. Y.T. Tran, J. Lee, P. Kumar, K.-H. Kim, S.S. Lee, Natural zeolite and its application in concrete composite production, *Composites Part B: Engineering*. 165 (2019) 354–364. https://doi.org/10.1016/j.compositesb.2018.12.084.